Journal of Medicinal Chemistry

Article

pubs.acs.org/jmc

Potent and Highly Selective Benzimidazole Inhibitors of PI3-Kinase Delta

Jeremy M. Murray,*[,†] Zachary K. Sweeney,*[,†] Bryan K. Chan,[†] Mercedesz Balazs,[†] Erin Bradley,[†] Georgette Castanedo,[†] Christine Chabot,[†] David Chantry,[†] Michael Flagella,[†] David M. Goldstein,[§] Rama Kondru,[§] John Lesnick,[†] Jun Li,[†] Matthew C. Lucas,[§] Jim Nonomiya,[†] Jodie Pang,[†] Stephen Price,[‡] Laurent Salphati,[†] Brian Safina,[†] Pascal P. A. Savy,[‡] Eileen M. Seward,[‡] Mark Ultsch,[†] and Daniel P. Sutherlin[†]

[†]Genentech, Inc., 1 DNA Way, South San Francisco, California 94080, United States

[‡]Argenta Discovery, 8/9 Spire Green Centre, Flex Meadow, Harlow CM19 5TR, United Kingdom

[§]Roche Research Center, 340 Kingsland Street, Nutley, New Jersey 07110, United States

Supporting Information

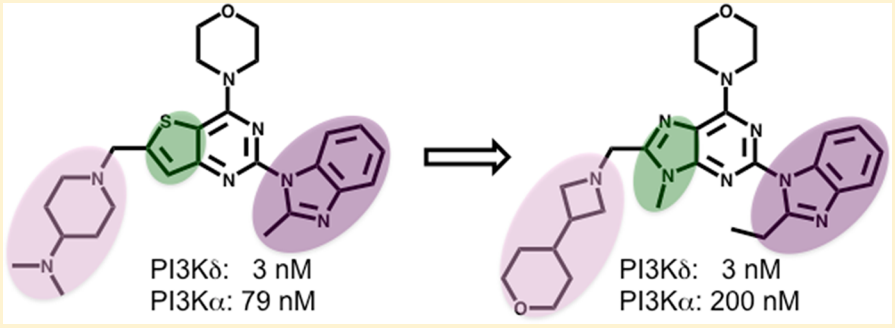

ABSTRACT: Inhibition of PI3Kδ is considered to be an attractive mechanism for the treatment of inflammatory diseases and leukocyte malignancies. Using a structure-based design approach, we have identified a series of potent and selective benzimidazole-based inhibitors of PI3Kδ. These inhibitors do not occupy the selectivity pocket between Trp760 and Met752 that is induced by other families of PI3Kδ inhibitors. Instead, the selectivity of the compounds for inhibition of PI3Kδ relative to other PI3K isoforms appears to be due primarily to the strong interactions these inhibitors are able to make with Trp760 in the PI3Kδ binding pocket. The pharmacokinetic properties and the ability of compound **5** to inhibit the function of B-cells in vivo are described.

INTRODUCTION

Phosphoinositide 3-kinase delta (PI3Kδ) participates in the activation of leukocytes by catalyzing the production of the cellular second messenger phosphatidylinositol-3,4,5-trisphosphate (PIP3). Mice that express a form of PI3Kδ that is catalytically inactive demonstrate deficient B-cell development and reduced production of T-cell dependent antibodies.[1,2] Inhibition of PI3Kδ is therefore considered to be an attractive mechanism for the treatment of inflammatory diseases and leukocyte malignancies.[3−5]

The class IA and class IB lipid kinases are structurally related and include PI3Kα, PI3Kβ, PI3Kδ, and PI3Kγ.[6] Several small molecules that inhibit the kinase activity of all members of the PI3K family, including 4-(2-(1*H*-indazol-4-yl)-6-((4-(methylsulfonyl)piperazin-1-yl)methyl)thieno[3,2-*d*]pyrimidin-4-yl)morpholine (GDC-0941)[7] (**1**, Figure 1), are currently in clinical trials for the treatment of cancer.[8,9] While these molecules have demonstrated efficacy in animal models,[10] the broad tissue distribution of PI3Kα and PI3Kβ and the apparently essential role that these enzymes play in embryonic development suggest that pan-PI3K inhibitors might have limited tolerability in the treatment of PI3Kδ driven disease. As such, there have been efforts directed toward the discovery of selective inhibitors of PI3Kδ.[11]

The p110 subunits of several PI3K isoforms have been structurally characterized.[12−14] Williams, Shokat, and co-workers described the ATP-binding site of this subunit as including a hinge pocket, an affinity pocket, and a hydrophobic region that lies below a nonconserved rim of the active site (Figure 2A). Most selective PI3Kδ inhibitors occupy a selectivity pocket between Trp760 and Met752 that is formed by the concerted movement of these residues.[13,15] However, a modestly potent and selective PI3Kδ inhibitor that interacts with residues near the nonconserved rim but does not induce the selectivity pocket has also been described.[12] Our group has

Received: May 22, 2012
Published: August 9, 2012

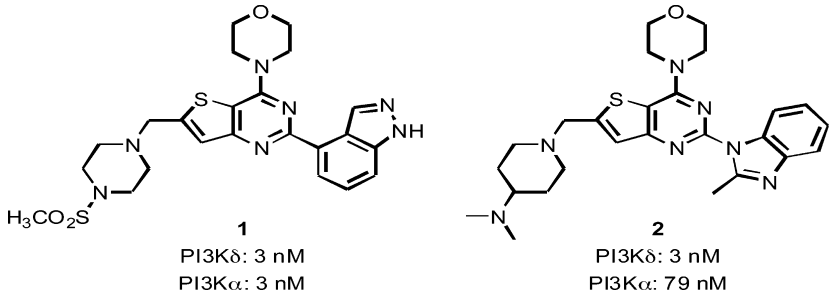

Figure 1. Structures of **1** (GDC-0941) and benzimidazole **2**.

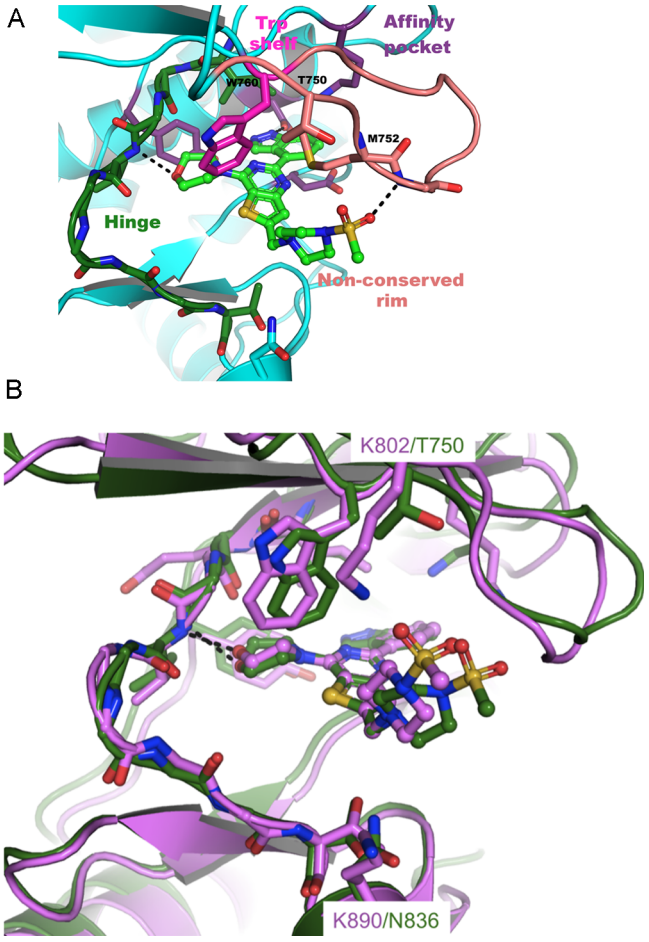

Figure 2. (A) Schematic of p110δ ATP-binding site illustrating important areas for inhibitor interactions. The figure is based on the crystal structure of p110δ in complex with GDC-0941 (**1**) (PDB ID 2WXP). GDC-0941 is colored green and shown as ball and sticks. The different regions are highlighted by labels of the corresponding colors. (B) Compound **1** (GDC-0941) bound to p110δ (PDB ID 2WXP, green) with an overlay of **1** bound to p110γ (PDB ID 1E8Y, violet). The nonconserved residues close to the inhibitor binding site are labeled.

recently reported that highly selective PI3Kδ inhibitors can be obtained by appropriate modification of heterocycles that occupy the affinity pocket of the PI3K enzymes.[16]

The pan-PI3K inhibitor **1** has a very similar binding mode in crystal structures of this inhibitor bound to p110δ and p110γ (Figure 2B).[6] The oxygen atom of the morpholine ring forms a hydrogen bond in the hinge region, while the sulfonylpiperazine adopts a dihedral angle of 60.5° relative to the plane defined by the thienopyrimidine ring and occupies a region that approaches the nonconserved rim (Figure 2A). In the affinity pocket, the indazole group makes hydrogen bond interactions with Asp787 from the kα3-helix and Tyr813 from kβ6. The poor δ/γ selectivity of this compound can be attributed to the broad distribution of the hydrophobic and electrostatic intermolecular interactions that are conserved across the various p110 isoforms.

In our previously reported work, benzimidazole **2** (Figure 1) was discovered to be a reasonably selective inhibitor of PI3Kδ (PI3Kα/PI3Kδ = 29).[16] Although **2** had modest in vitro permeability (MDCK A/B = 3×10^{-6} cm/s), it appeared to be a promising candidate for further optimization. In particular, we were encouraged that the benzimidazole inhibitors generally demonstrated good potency in cellular assays and had low potential for time-dependent inactivation of cytochrome p450 enzymes. The goal of the research described in this report was to identify benzimidazole-based inhibitors of PI3Kδ with improved selectivity against other PI3K isoforms as well as improved in vitro and in vivo pharmacokinetic properties.[17]

We first examined the effect of the central bicyclic ring on PI3Kδ and PI3Kα potency utilizing structure–activity relationships developed from earlier studies. In particular, we hypothesized that modification of the central heterocycle would allow us to adjust the interaction of the piperidine region of the inhibitors with Trp760 and residues located on the nonconserved rim of the binding pocket. This would allow us to specifically target the space created by the Thr750 side chain in p110δ, which is electronically and structurally distinct from the residues found in p110α, β, and γ (Arg770, Lys777, and Lys802, respectively). Although Trp760 is conserved across the different isoforms, the residues that interact with Trp760 are not. For example, the hydrophobic surface of Trp760 is likely to be *less* accessible in PI3Kα because in this isoform, the corresponding Trp residue (Trp780) is engaged in π-stacking or cation-π interactions with Arg770. Additionally, in PI3Kα, there is a hydrogen bond interaction between the indole ring of Trp780 and Glu789 on the kβ5 strand that might limit the mobility of the tryptophan ring.[13] Taken together, these interactions are likely to limit the access of small molecule inhibitors to the hydrophobic face of the tryptophan ring in PI3Kα. We were therefore particularly intrigued by the prospect of improving the ability of our inhibitors to selectively inhibit PI3Kδ by optimizing interactions with Trp760.

All compounds were tested in a biochemical assay that measured the inhibition of phosphatidylinositol-3,4,5-trisphosphate (PIP3) production by recombinant PI3K isoforms and in a cellular assay that monitored inhibition of phosphorylation of AKT in a Ri-1 cell line.[18] For this study, we chose to incorporate a piperidinyl-propan-2-ol group in place of the dimethylpiperidinamine group contained in **2**, as we reasoned

dx.doi.org/10.1021/jm300717c | J. Med. Chem. 2012, 55, 7686–7695

that replacement of the basic dimethylamino group should reduce inhibitor promiscuity and improve measured permeability.[19] This substitution did not sufficiently influence inhibitor potency or PI3Kα/PI3Kδ selectivity (i.e., **2** vs **3**). As shown in Table 1, most of the benzimidazole compounds initially prepared are potent inhibitors of PI3Kδ and feature some selectivity against the α-isoform. Heterocycles that contain a nitrogen atom instead of a sulfur atom in the 5-position of the pyrimidine ring are generally more selective and more potent inhibitors of PI3Kδ. Compound **8**, in which the position of the methylene linker is more dramatically shifted relative to lead compound **2** was significantly less effective than the other analogues. These observations are consistent with the hypothesis that movement of the piperidine group closer to Trp760 might increase selectivity for inhibition of PI3Kδ. Purines **4** and **5** are particularly interesting analogues, as these inhibitors maintain good potency in the cellular assay. Most encouragingly, additional profiling of **5** revealed that this compound is essentially inactive against PI3Kγ (IC_{50} > 10 μM, γ/δ > 5000) and only a weak inhibitor of PI3Kβ (IC_{50} = 547 nM, β/δ = 228).

Table 1. Inhibition of PI3Kδ Activity by Analogues 3−8

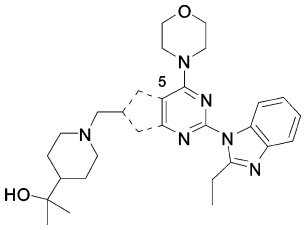

Compound	Ring	$IC_{50}\delta$ [a]	$IC_{50}\alpha/IC_{50}\delta$	IC_{50} pAKT
3	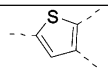	5	19	116
4	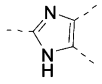	3	46	12
5	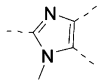	2	84	14
6	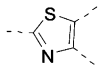	10	38	7
7	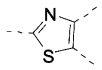	1	52	50
8	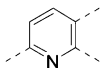	>1000	-	-

[a]Inhibition of phosphatidylinositol-3,4,5-trisphosphate (PIP3) production by recombinant PI3Kδ (nM).

Further analysis of the calculated ground state conformation of **5** indicated that this inhibitor may adopt a low-energy conformation in which the purine and benzimidazole rings are coplanar. In order to determine if restriction of the torsional angle between these heterocycles would influence inhibitor selectivity or improve the physical properties of these compounds, we prepared a series of analogues with bulky groups attached to the C(2) position of the benzimidazole ring (Table 2). Ab initio calculations[20] suggested that bulky groups at the C(2)-position of the benzimidazole would strongly disfavor coplanarity of the aromatic heterocycles.

Table 2. Inhibition of PI3Kδ Activity by Analogues 9−15

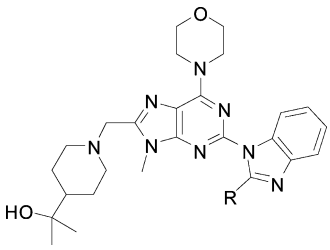

Compound	R	$IC_{50}\delta$ [a]	$IC_{50}\alpha/IC_{50}\delta$	IC_{50} pAKT
9		4	99	-
10		2	101	10
11		3	90	19
12		5	75	17
13		2	60	19
14		6	60	16
15		39	10	-

[a]Inhibition of phosphatidylinositol-3,4,5-trisphosphate (PIP3) production by recombinant PI3Kδ (nM).

In general, branched substituents at the C(2) position of the benzimidazole were accommodated by both PI3Kα and PI3Kδ isoforms (Table 2). Incorporation of larger groups, such as the morpholine ring found in **15**, reduced inhibition of PI3Kδ. Generally, a small variation in isoform selectivity was observed for inhibitors in this series, although some compounds with excellent selectivity and activity in the cellular assay were identified (e.g., ether **10**).

Structural characterization of **14** bound to p110γ[21] showed that there is a significant (32°) torsional angle between the benzimidazole and purine rings in the bound conformation (Figure 3). The benzimidazole ring engages in hydrogen-bonding interactions with Lys833, while the dimethyl amino group is twisted relative to the plane of the benzimidazole. One of the methyl groups of the dimethylamine unit occupies a small hydrophobic pocket formed by Pro810 and Lys833.

The piperidine ring of **14** engages in the targeted hydrophobic contacts with Trp812 (Trp760 in p110δ). The observed location of the piperidine ring of **14** is strikingly different from that found for the analogous sulfonylpiperazine group of **1** in cocrystal structures with p110γ (**14**, dihedral angle =157°, Figure 3; **1**, dihedral angle = 60°, Figure 2A) The sulfonyl oxygen atoms of **1** contact the NH_3 of Lys802 and the backbone amide of Ala805. The isopropanol unit of **14** is likely to be unable to interact productively with these residues and instead shifts to form weak hydrophobic interactions with

dx.doi.org/10.1021/jm300717c | J. Med. Chem. 2012, 55, 7686−7695

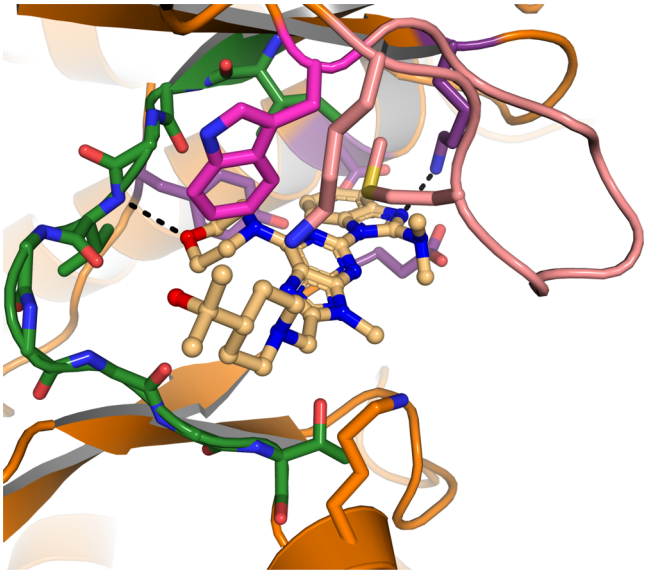

Figure 3. Co-crystal structure of **14** and p110γ (PDB-ID 4GB9). The dihedral angle between the plane formed by the purine ring and the piperidine ring is 157°. The hydrogen bond interactions between Val882 in the hinge and Lys833 of the affinity pocket are represented as black dotted lines.

Trp812. The resulting suboptimal fit is likely to be partly responsible for the modest potency of **14** against PI3Kγ (IC_{50} = 540 nM). As anticipated, substitution of the 4-(propan-2-ol)-piperidine subunit of **5** with the 4-methanesulfonylpiperazine unit of **1** (**5** to **16**, Table 3) resulted in a significant increase in activity versus PI3Kα and PI3Kγ. These structure–activity relationships highlight the crucial role of the amine subunit in determining PI3K isoform selectivity for this series of inhibitors.

Further optimization focused on replacement of the 4-(propan-2-ol)-piperidine subunit of **5** with alternative sterically demanding amines. Compounds containing a hydrophobic group attached to the piperazine ring (**18**, Table 3), bulky amine groups (**19**), and azetidine compounds (**20**) were also potent, selective PI3K-δ inhibitors. A docking model of **19**[22] (Figure 4) suggests that several methylene groups of the bicycloheptane unit form favorable packing interactions with the indole ring of Trp760. In summary, the structure–activity relationship of these inhibitors provide further evidence that high PI3K isoform selectivity can be achieved for structurally diverse PI3Kδ inhibitors that do not occupy the selectivity pocket formed by the movement of Met752 and Trp760. These inhibitors instead exploit residue differences close to Trp760 that influence the ability to make favorable interactions with this residue in PI3Kδ but not in the other PI3K isoforms.[12,13]

Benzimidazoles **5** and **20** are generally representative of this series of inhibitors and were selected for further profiling. Inhibitor **20** is soluble in aqueous solution (sol. at pH 6.5 = 338 μg/mL) and has good permeability in a standard MDCK assay (P_{app} = 16 × 10^{-6} cm/s). Rat (90%) and human (91%) plasma protein binding was moderate. There was no reversible or time-dependent CYP inhibition associated with **20** in testing against five CYP isoforms.[23] In addition, very weak inhibition with (less than 25% inhibition at 1 μM) was observed in testing against a panel of 55 diverse kinases.[24] Similar results were obtained for compound **5**. Pharmacokinetic profiling of compounds **5** and **20** in rat and dog indicated that **5** has moderate to low clearance in both species, while **20** is cleared more rapidly in the rat (Table 4).

Table 3. Inhibition of PI3Kδ Activity by Benzimidazole Analogues 5 and 16–20

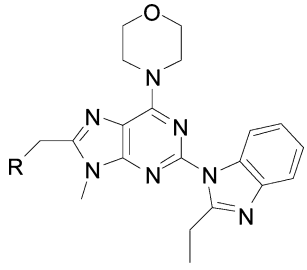

Compound	R	$IC_{50}\delta$[a]	$IC_{50}\alpha/IC_{50}\delta$	$IC_{50}\gamma/IC_{50}\delta$
5	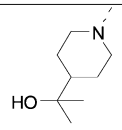	2	84	>5000
16	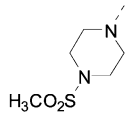	6	5	20
17	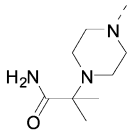	2	56	140
18	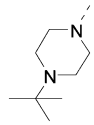	1	120	1350
19	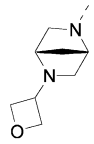	3	160	280
20	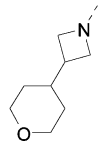	2	100	260

[a]Inhibition of phosphatidylinositol-3,4,5-trisphosphate (PIP3) production by recombinant PI3Kδ (nM).

B-lymphocyte signaling plays a critical role in many inflammatory diseases. We therefore chose to investigate if our PI3Kδ-selective inhibitors could influence B-cell activation in vivo. Activation of mouse spleen B-cells by anti-IgD stimulates the expression of CD86 on the surface of B cells, which can be quantified ex vivo by FACS analysis.[25] To test if PI3Kδ inhibitors might modulate the induced CD86 expression, compound **5** was orally administered to rats. After 30 min, anti-IgD was injected. Analysis of the percentage of B-cells from the spleen that expressed CD86 after anti-IgD treatment revealed that compound **5** could significantly inhibit B-cell activation following oral doses as low as 1 mg/kg (Figure 5).

dx.doi.org/10.1021/jm300717c | J. Med. Chem. 2012, 55, 7686–7695

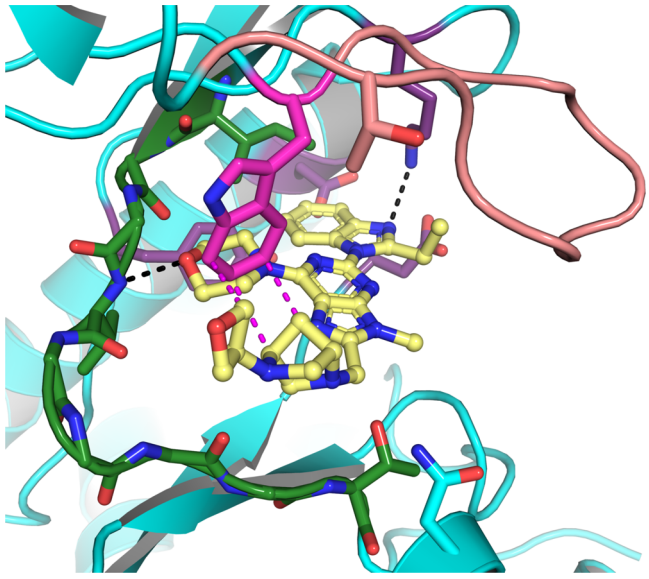

Figure 4. Model of **19** bound to p110δ. The possible hydrophobic interaction between the bicycloheptane ring and Trp760 is represented by the magenta dashed lines.

Table 4. Pharmacokinetic Parameters for Inhibitors 5 and 20 in Rat and Dog

compd	species	Cl[a]	Vd_{ss} (L/kg)	$T_{1/2}$ (h)	F %
5	rat	19	4.1	1.5	92
	dog	5	2	6.4	>100
20	rat	34	6.5	2.6	
	dog	25	6.5	3.6	56

[a]Reported as mL/min/kg.

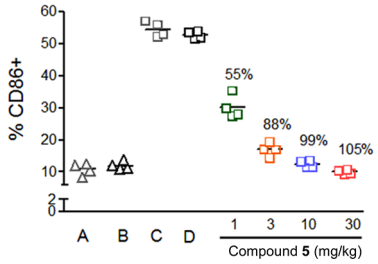

Figure 5. Compound **5** inhibits the activation of B-cells, as measured by CD86 expression, following anti-IgD stimulation. A: Saline. B: MCT. C: anti-IgD + saline. D: anti-IgD + MCT.

Inhibitors **3**–**7** were synthesized according to the general process as depicted in Scheme 1. Treatment of pyrimidines **21**–**25** with morpholine yielded tricyclic intermediates **26**–**30**.[15] Deprotonation of tricycles **26**–**30** with *n*-butyllithium followed by quenching with *N*,*N*-dimethylformamide afforded the corresponding aldehydes **31**–**35**. Reductive amination of **31**–**35** using 4-(2-propanol)-piperidine then generated compounds **36**–**40**. Alternatively, this transformation can be achieved through a three-step sequence that includes reduction, bromination and alkylation. The palladium-catalyzed coupling of 2-chloropyrimidines **36**–**40** and 2-ethylbenzimidazole then afforded compounds **3**, **5**–**7**, and **41**. Treatment of **41** with acid generated inhibitor **4**. Analogous procedures were used for the preparation of inhibitors **16**–**18** and **20**. In a similar fashion, the synthesis of inhibitor **19** was completed as outlined in Scheme 2.

Scheme 1[a]

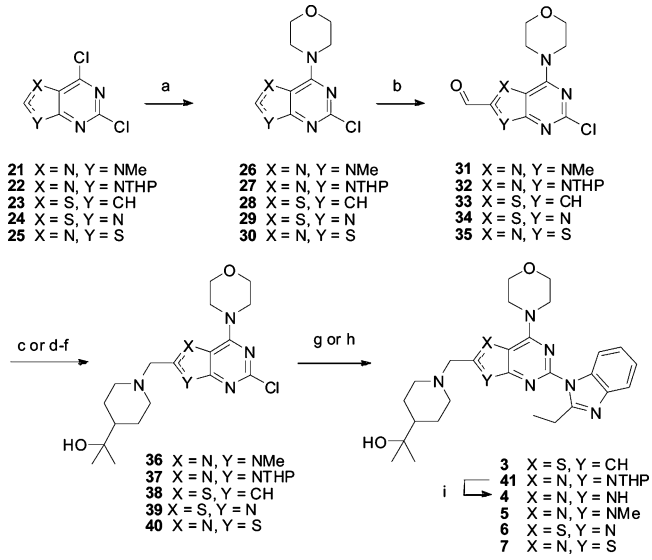

[a]Reagents and conditions: (a) morpholine, DCM, 0 °C to rt, 1–24 h; (b) *n*-BuLi, THF, −78 °C, 1 h then DMF, −78 °C, 30 min; (c) 4-(2-propanol)-piperidine, $NaHB(OAc)_3$, MS 4 Å, DCE, 20 h; (d) $NaBH_4$, MeOH, 0 °C, 1 h; (e) PBr_3, DCM, 1 h; (f) 4-(2-propanol)-piperidine, DIEA, DCM, 1–2 h; (g) 2-ethylbenzimidazole, Cs_2CO_3, $Pd_2(dba)_3$, XPhos, 1,4-dioxane, 140 °C, microwave, 20–30 min; (h) 2-ethylbenzimidazole, Cs_2CO_3, copper(I) thiophene-2-carboxylate, NMP, 110 °C, 18 h; (i) PTSA, MeOH, 40 °C, 24 h.

Compounds **9**–**11** and **13**–**15** were synthesized by coupling of **36** and the corresponding C(2)-substituted benzimidazoles (Scheme 3). Compound **12** was prepared through the palladium-catalyzed coupling of **36** with phenylene-1,2-diamine to provide intermediate **45**. Treatment of **45** with refluxing (±)-lactic acid provided pure **12** following HPLC and SFC purification.

This report describes the identification of a new family of highly selective PI3Kδ inhibitors. Representative compounds have good selectivity versus other PI3K isoforms, promising physical properties, and anti-inflammatory properties in vivo. The structural information disclosed supports the hypothesis that PI3K-isoform selectivity can be achieved with inhibitors that do not occupy the induced pocket between Trp760 and Met752 in PI3Kδ. Improvements in the selectivity and pharmacokinetic properties of this series of PI3K inhibitors will be the subject of future reports.

EXPERIMENTAL SECTION

All solvents and reagents were used as obtained. ^{1}H NMR spectra were recorded with a Bruker Avance DPX400 Spectrometer or a Varian Inova 400 NMR spectrometer and referenced to tetramethylsilane. Chemical shifts are expressed as δ units using tetramethylsilane as the external standard (in NMR description, s, singlet; d, doublet; t, triplet; q, quartet; m, multiplet; and br, broad peak). All coupling constants (J) are reported in Hertz. Mass spectra were measured with an Agilent quadrupole 6140 spectrometer using an ESI source coupled to an Agilent 1200 HPLC system operating in reverse mode with an Agilent SD-C18 (30 mm by 2.1 mm) with 1.8 μm sized particles. Analytical purities of evaluated compounds were >95% unless stated otherwise. The following analytic method was used, unless stated otherwise: HPLC Agilent 1200, water with 0.05% TFA, acetonitrile with 0.05% TFA, Agilent Zorbax SD-C18, 1.8 μM, 2.1 mm × 30 mm, 40 °C, 3–95% B in 8.5 min, 95% in 2.5 min, 400 μL/min, 220 and 254 nm, equipped with Agilent quadrupole 6140, ESI positive, and 110–800

dx.doi.org/10.1021/jm300717c | J. Med. Chem. 2012, 55, 7686–7695

Scheme 2[a]

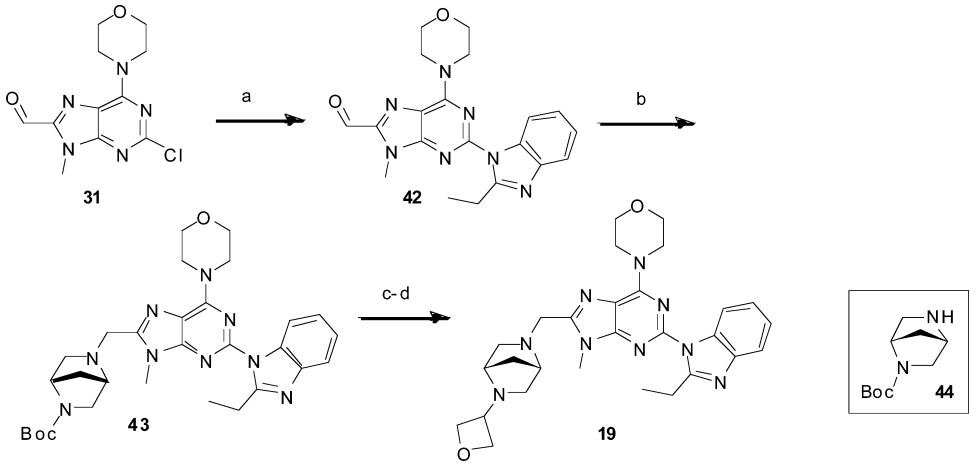

[a]Reagents and conditions: (a) 2-ethylbenzimidazole, Cs_2CO_3, $Pd_2(dba)_3$, XPhos, 1,4-dioxane, 140 °C, microwave, 20−30 min; (b) **44**, $NaHB(OAc)_3$, MS 4 Å, DCE, 20 h; (c) TFA, DCM, 30 min; (d) oxetan-3-one, $NaHB(OAc)_3$, MS 4 Å, DCE, 20 h.

Scheme 3[a]

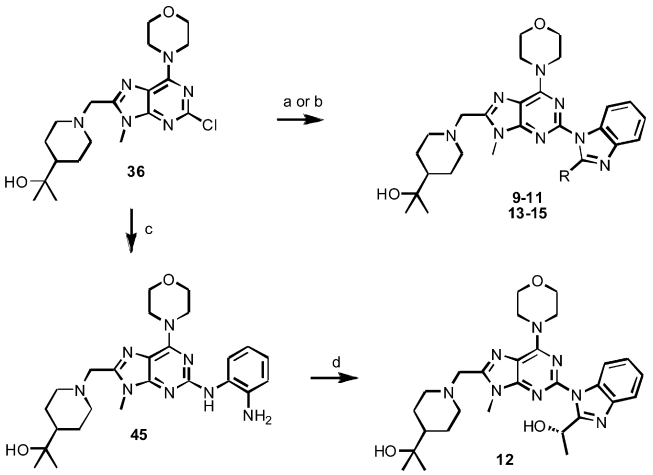

[a]Reagents and conditions: (a) benzimidazole, Cs_2CO_3, $Pd_2(dba)_3$, XPhos, DMF, 140 °C, microwave, 20−30 min; (b) benzimidazole, NaO^tBu, $(^tBu_3P)_2Pd$, $Pd(OAc)_2$, toluene, 140 °C, microwave, 30 min; (c) 1,2-phenylenediamine, $Pd_2(dba)_3$, XPhos, DMF, 140 °C, microwave, 30 min; (d) (±)-lactic acid, 125 °C.

amu. Microwave reactions were performed using a Biotage Initiator Reactor.

Preparation of Compounds 26−30. Compounds **26−30** were prepared according to a similar procedure previously described in ref 17 and references therein. Briefly, a mixture of the dichloropyrimidine (**21−25**, 1.0 mmol) and morpholine (2.5 mmol) in MeOH (80 mL) was stirred at 0 °C for 0.5 h. The mixture was then allowed to warm to room temperature and stirred for 1.5 h. The solvent was evaporated. The residue was redissolved in DCM and washed successively with 1 M HCl and brine, dried over Na_2SO_4, filtered, and concentrated to give **26−30** (yield 96−99%).

Preparation of 2-(1-((2-(2-Ethyl-1*H*-benzo[*d*]imidazol-1-yl)-9-methyl-6-morpholino-9*H*-purin-8-yl)methyl)piperidin-4-yl)-propan-2-ol (5). To a solution of **26** (10.0 g, 39.4 mmol) and *N*,*N*,*N*′*N*′-tetramethylethylenediamine (9.0 mL) in THF (200 mL) at −78 °C was added a 2.5 M solution of *n*-butyllithium in THF (35 mL, 87.5 mmol). The solution was stirred at −40 °C for 30 min and then recooled to −78 °C, whereupon DMF (8 mL) was added, and the reaction was stirred for another hour. The reaction was quenched into a cold 0.25 N HCl solution via 10 mL serological pipet aliquots. Ice was added to keep the quenching solution temperature below 5 °C. The resulting precipitate was collected by filtration to afford **31** as a light yellow solid (11 g, 99%).

To a solution of **31** (0. 50 g, 2.0 mmol) in 1,2-dichloroethane (16 mL) was added 4-(propan-2-ol)-piperidine (0.254 g, 1.77 mmol), micronized 4 Å molecular sieves (1.5 g), and *N*,*N*-diisopropylethylamine (0.68 mL, 3.9 mmol). The resulting mixture was stirred at room temperature for 2 h prior to the addition of sodium triacetoxyborohydride (0.752 g, 3.55 mmol). The reaction was deemed complete after stirring at room temperature for 20 h. The reaction mixture was filtered and concentrated. The residue was purified by flash chromatography (0−10% MeOH gradient in DCM) to give intermediate **36** (1.56 g, 89.6%).

Alternatively, **36** can be synthesized as follows: To a solution of **31** (15.0 g, 53.3 mmol) in MeOH (700 mL) was added sodium borohydride (10.1 g, 266 mmol) at 0 °C. The reaction was then allowed to warm to room temperature and stirred for 30 min. The reaction mixture was reduced to approximately 1/3 of its volume under vacuum. To the mixture was added 0.5 L of a 1:1 (v/v) mixture of saturated sodium bicarbonate and water. The aqueous mixture was extracted with EtOAc. The combined organic extracts were washed with water and dried over $MgSO_4$, filtered, and concentrated to a white solid.

The solid was then dissolved in a mixture of 1,2-dichloroethane (320 mL) and THF (250 mL) and cooled to 0 °C. To the cooled mixture was slowly added PBr_3 (8.7 mL, 93 mmol) to give a slurry. After stirring at 0 °C for 1 h, the cold reaction mixture was filtered to collect the solid. The solid was washed with 50 mL of a 1:1 (v/v) mixture of water and saturated sodium bicarbonate and 150 mL of water. The washed residue was then suspended in 80 mL of a 1:4 mixture of MeOH and water. The solid was collected by filtration and air-dried to give 4-(8-(bromomethyl)-2-chloro-9-methyl-9*H*-purin-6-yl)morpholine as a white solid (12.8 g).

A portion of the white solid (2.0 g) was then redissolved in DCM (48 mL) and to the solution was added 4-(propan-2-ol)-piperidine (0.827 g, 5.77 mmol) and *N*,*N*-diisopropylethylamine (1.5 mL, 8.7 mmol). The reaction was then stirred at room temperature for 18 h prior to dilution with water. The aqueous mixture was extracted three times with DCM. The combined extracts were washed with water, dried over Na_2SO_4, filtered, and concentrated to give **36** (17 g, 78%).

To a microwave tube was added **36** (2.0 g, 4.89 mmol), 2-ethyl-1*H*-benzo[*d*]imidazole (715 mg, 4.89 mmol), cesium carbonate (3.19 g, 9.78 mmol), tris(dibenzylideneacetone)dipalladium (305 mg, 0.333 mmol), XPhos (305 mg, 0.640 mmol), and DMF (37 mL). The reaction was heated at 145 °C for 30 min in the microwave. The reaction was then cooled to room temperature, diluted with EtOAc, filtered through Celite, and concentrated. The crude product was then purified by flash chromatography (0−10% MeOH gradient in DCM)

dx.doi.org/10.1021/jm300717c | J. Med. Chem. 2012, 55, 7686−7695

followed by reverse phase HPLC to give **5** (1.8 g, 71%) as a white solid. ^{1}H NMR (400 MHz, DMSO-d_6) δ 8.01 (m, 1H), 7.62 (m, 1H), 7.26 (m, 2H), 4.25 (s, br, 4H), 4.02 (s, 1H), 3.81 (s, 3H), 3.77 (m, 4H), 3.73 (s, 2H), 3.28 (m, 2H), 2.90 (d, J = 10.9, 2H), 1.99 (m, 2H), 1.66 (d, J = 10.8, 2H), 1.34 (t, J = 7.43, 3H), 1.19 (m, 3H), 1.02 (s, 6H). MS (ESI): m/z (M + H)$^+$ 519. Analytical LC-MS on an Agilent 1200 using a 2.1 mm × 30 mm SD-C18 analytical column and H_2O/MeCN modified with 0.05% trifluoroacetic acid, running a linear gradient from 3% MeCN to 95% MeCN, monitoring by a UV wavelength of 254 nm and ESI+ TIC MS, showed 100% purity.

Preparation of 2-(1-((2-(2-Ethyl-1*H*-benzo[*d*]imidazol-1-yl)-6-morpholino-9*H*-purin-8-yl)methyl)piperidin-4-yl)propan-2-ol (4). Compound **41** was prepared from **22** according to a procedure similar to that described for compound **5**. Compound **41** was then treated with equimolar of *p*-toluenesulfonic acid in methanol at 40 °C for 24 h. The reaction was then concentrated, and **4** was isolated by reverse phase HPLC purification. Yield = 38%. ^{1}H NMR (400 MHz, DMSO-d_6) δ 7.96 (m, 1H), 7.62 (m, 1H), 7.23 (m, 2H), 4.24 (s, br, 4H), 4.02 (s, 1H), 3.77 (m, 4H), 3.64 (s, 2H), 3.25 (m, 2H), 2.91 (d, J = 11.1, 2H), 1.00 (t, J = 10.9, 2H), 1.65 (d, J = 11.7, 2H), 1.30 (t, J = 11.1, 3H), 1.12−1.30 (m, 3H), 1.02 (s, 6H). MS (ESI): m/z (M + H)$^+$ 505. Analytical LC-MS on an Agilent 1200 using a 2.1 mm × 30 mm SD-C18 analytical column and H_2O/MeCN modified with 0.05% trifluoroacetic acid, running a linear gradient from 5% MeCN to 100% MeCN, monitoring by a UV wavelength of 254 nm and ESI+ TIC MS, showed 100% purity.

Preparation of 2-(1-((2-(2-ethyl-1*H*-benzo[*d*]imidazol-1-yl)-4-morpholinothieno[3,2-*d*]pyrimidin-6-yl)methyl)piperidin-4-yl)propan-2-ol (5). Compound **3** was prepared from **23** according to a procedure similar to that described for compound **5**. Yield = 42%. ^{1}H NMR (400 MHz, DMSO-d_6) δ 8.00 (m, 1H), 7.65 (m, 1H), 7.42 (s, 1H), 7.25 (m, 2H), 4.07 (s, 1H), 3.97 (m, 4H), 3.83 (s, 2H), 3.81 (m, 4H), 3.27 (m, 2H), 2.99 (d, J = 10.9, 2H), 1.99 (t, J = 11.3, 2H), 1.67 (d, J = 11.3, 2H), 1.32 (t, J = 7.43, 3H), 1.11−1.29 (m, 3H), 1.04 (s, 6H). MS (ESI): m/z (M + H)$^+$ 521. Analytical LC-MS on an Agilent 1200 using a 2.1 mm × 30 mm SD-C18 analytical column and H_2O/MeCN modified with 0.05% trifluoroacetic acid, running a linear gradient from 5% MeCN to 100% MeCN, monitoring by a UV wavelength of 254 nm and ESI+ TIC MS, showed 99.8% purity.

Preparation of 2-{1-[5-(2-Ethylbenzoimidazol-1-yl)-7-morpholin-4-yl-thiazolo[4,5-*d*]pyrimidin-2-ylmethyl]piperidin-4-yl}propan-2-ol (6). Compound **6** was prepared from **24** according to a procedure similar to that described for compound **3**. Yield = 37%. ^{1}H NMR (400 MHz, $CDCl_3$): δ 8.11 (1H, m), 7.77−7.70 (1H, m), 7.23 (2H, m), 4.01−3.99 (6H, m), 3.87 (5H, m), 3.42−3.39 (2H, m), 3.10 (2H, m), 2.27 (2H, m), 1.79 (2H, m), 1.50 (2H, m), 1.46−1.40 (3H, m), 1.32 (1H, m), 1.20 (6H, s). MS (ESI): m/z (M + H)$^+$ 522. Analytical LC-MS on an Agilent 1200 using a 2.1 mm × 30 mm SD-C18 analytical column and H_2O/MeCN modified with 0.05% trifluoroacetic acid, running a linear gradient from 5% MeCN to 100% MeCN, monitoring by a UV wavelength of 254 nm and ESI+ TIC MS, showed 97.3% purity.

Preparation of 2-{1-[5-(2-Ethylbenzoimidazol-1-yl)-7-morpholin-4-yl-thiazolo[5,4-*d*]pyrimidin-2-ylmethyl]piperidin-4-yl}propan-2-ol (7). Compound **40** was first prepared from **25** according to a procedure similar to that described for compound **3**. A mixture of **40** (100 mg, 0.24 mmol), 2-ethyl-1*H*-benzimidazole (42 mg, 0.29 mmol), copper(I) thiophene-2-carboxylate (9 mg, 0.048 mmol), and cesium carbonate (119 mg, 0.36 mmol) in NMP (0.5 mL) was then stirred at 110 °C for 18 h. The reaction mixture was diluted with MeOH and loaded onto an Isolute SCX-2 cartridge (5 g). The cartridge was washed with MeOH, and the desired product was eluted with 2 M NH_3 in MeOH. The solvents were removed, and the residue was subjected to flash chromatography (0−20% MeOH in EtOAc) followed by reverse phase HPLC to give the title compound as a beige solid (45 mg, 36%). ^{1}H NMR (400 MHz, $CDCl_3$): δ 8.03−7.98 (m, 1H); 7.77−7.73 (m, 1H); 7.32−7.24 (m, 2H); 4.41 (m, 4H); 3.90−3.85 (m, 6H); 3.35 (q, J = 7.5, 2H); 3.11 (m, 2H); 2.33−2.12 (m, 2H); 1.79 (m, 2H); 1.57 (m, 2H); 1.44 (t, J = 7.5, 3H); 1.34 (m, 1H); 1.22 (s, 6H). MS (ESI): m/z (M + H)$^+$ 522. Analytical LC-MS on an Agilent 1200 using a 2.1 mm × 30 mm SD-C18 analytical column and H_2O/MeCN modified with 0.05% trifluoroacetic acid, running a linear gradient from 3% MeCN to 95% MeCN, monitoring by a UV wavelength of 254 nm and ESI+ TIC MS, showed 99% purity.

Preparation of 2-(1-((9-Methyl-6-morpholino-2-(2-(tetrahydrofuran-2-yl)-1*H*-benzo[*d*]imidazol-1-yl)-9*H*-purin-8-yl)methyl)piperidin-4-yl)propan-2-ol (9). To a microwave tube was charged **36** (65 mg, 0.16 mmol), 2-(tetrahydrofuran-2-yl)-1*H*-benzo[*d*]imidazole (61 mg, 0.323 mmol), palladium diacetate (5.4 mg, 0.024 mmol), bis(tri*tert*-butylphosphine)palladium (12 mg, 0.024 mmol) and sodium *tert*-butoxide (31 mg, 0.32 mmol). The tube was flushed with nitrogen for 5 min prior to the addition of toluene (2.6 mL). The reaction was then sealed and heated to 145 °C for 30 min in a microwave. The reaction mixture was diluted with MeOH and loaded onto a Biotage Isolute SCX-2 column. The column was washed with MeOH followed by elution of the desired product by the addition of a 2 M ammonia solution in methanol. After concentration, the crude product was purified by reverse phase HPLC to give the title compound (35 mg, 39%). ^{1}H NMR (400 MHz, DMSO-d_6) δ 7.99 (dd, J = 6.99, J = 1.75, 1H), 7.70 (dd, J = 6.79, J = 1.76, 1H), 7.29 (m, 2H), 5.88 (m, 1H), 4.25 (s, br, 4H), 4.02 (s, 1H), 3.80−3.85 (m, 4H), 3.77 (m, 4H), 3.73 (s, 2H), 2.91 (d, J = 11.4, 2H), 2.53−2.59 (m, 1H), 2.26−2.33 (m, 1H), 1.90−2.09 (m, 4H), 1.66 (d, J = 11.1, 2H), 1.14−1.26 (m, 3H), 1.02 (s, 6H). MS (ESI): m/z (M + H)$^+$ 561. Analytical LC-MS on an Agilent 1200 using a 2.1 mm × 30 mm SD-C18 analytical column and H_2O/MeCN modified with 0.05% trifluoroacetic acid, running a linear gradient from 3% MeCN to 95% MeCN, monitoring by a UV wavelength of 254 nm and ESI+ TIC MS, showed 100% purity.

Preparation of 2-(1-((2-(2-(1-Methoxyethyl)-1*H*-benzo[*d*]-imidazol-1-yl)-9-methyl-6-morpholino-9*H*-purin-8-yl)methyl)-piperidin-4-yl)propan-2-ol (10). To a microwave tube was charged **36** (0.15 g, 0.37 mmol), 2-(1-methoxyethyl)-1*H*-benzo[*d*]imidazole (0.097 g, 0.55 mmol), tris(dibenzylideneacetone)dipalladium(0) (23 mg, 0.025 mmol), XPhos (23 mg, 0.048 mmol), cesium carbonate (0.24 g, 0.73 mmol), and DMF (3 mL). The reaction was then sealed and heated to 145 °C for 20 min in a microwave. The reaction was then concentrated, and the crude product was purified by reverse phase HPLC to give the title compound (160 mg, 29.7%). ^{1}H NMR (400 MHz, DMSO-d_6) δ 7.95 (m, 1H), 7.70 (m, 1H), 7.28 (m, 2H), 5.42 (m, 1H), 4.28 (s, br, 4H), 4.00 (s, 1H), 3.82 (s, 3H), 3.76 (m, 4H), 3.74 (s, 2H), 3.09 (s, 3H), 2.97 (m, 2H), 2.00 (m, 2H), 1.67 (m, 4H), 1.19 (m, 2H), 1.02 (s, 6H), 0.92 (m, 1H). MS (ESI): m/z (M + H)$^+$ 549. Analytical LC-MS on an Agilent 1200 using a 2.1 mm × 30 mm SD-C18 analytical column and H_2O/MeCN modified with 0.05% trifluoroacetic acid, running a linear gradient from 3% MeCN to 95% MeCN, monitoring by a UV wavelength of 254 nm and ESI+ TIC MS, showed 100% purity.

Preparation of 2-(1-((2-(2-Cyclopropyl-1*H*-benzo[*d*]-imidazol-1-yl)-9-methyl-6-morpholino-9*H*-purin-8-yl)methyl)-piperidin-4-yl)propan-2-ol (11). To a microwave tube was charged **36** (0.415 g, 1.01 mmol), 2-cyclopropyl-1*H*-benzo[*d*]imidazole (0.200 g, 1.26 mmol), tris(dibenzylideneacetone)dipalladium(0) (28 mg, 0.030 mmol), XPhos (29 mg, 0.061 mmol), cesium carbonate (0.661 g, 2.0 mmol) and DMF (5 mL). The reaction was then heated to 140 °C for 30 min in a microwave. The reaction mixture was diluted with MeOH and loaded onto a Biotage Isolute SCX-2 column. The column was washed with MeOH followed by elution of the desired product by the addition of a 2 M ammonia solution in methanol. After concentration, the crude product was purified by reverse phase HPLC to give the title compound (160 mg, 29.7%). ^{1}H NMR (400 MHz, DMSO-d_6) δ 7.95 (m, 1H), 7.56 (m, 1H), 7.21 (m, 2H), 4.26 (s, br, 4H), 4.02 (s, 1H), 3.82 (s, 3H), 3.77 (m, 4H), 3.74 (s, 2H), 2.89 (m, 3H), 2.00 (t, J = 10.7, 2H), 1.66 (d, J = 10.4, 2H), 1.05−1.30 (m, 7H), 1.02 (s, 6H). MS (ESI): m/z (M + H)$^+$ 531. Analytical LC-MS on an Agilent 1200 using a 2.1 mm × 30 mm SD-C18 analytical column and H_2O/MeCN modified with 0.05% trifluoroacetic acid, running a linear gradient from 3% MeCN to 95% MeCN, monitoring by a UV wavelength of 254 nm and ESI+ TIC MS, showed 96% purity.

Preparation of 2-(1-((2-(2-(1-Hydroxyethyl)-1*H*-benzo[*d*]-imidazol-1-yl)-9-methyl-6-morpholino-9*H*-purin-8-yl)methyl)-piperidin-4-yl)propan-2-ol (12). To a microwave tube was charged

dx.doi.org/10.1021/jm300717c | *J. Med. Chem.* 2012, 55, 7686−7695

36 (2.2 g, 5.42 mmol), phenylene-1,2-diamine (0.73 g, 6.78 mmol), tris(dibenzylideneacetone)dipalladium(0) (0.39 g, 0.43 mmol), XPhos (0.41 g, 0.87 mmol), cesium carbonate (3.54 g, 10.9 mmol), and DMF (42 mL). The reaction was then sealed and heated to 140 °C for 40 min in a microwave. The reaction mixture was allowed to cool to room temperature and filtered. The filtrate was then concentrated to give compound **45** as a purple solid (3.2 g). This crude material was used in the following step without further purification.

Crude **45** (0.53 g) was combined with (±)-lactic acid (4 mL) and heated to 125 °C in a sealed vessel for 3.5 h. The reaction mixture was cooled to room temperature and concentrated. The crude product was purified by reverse phase HPLC. The enantiomers were separated by chiral SFC to give **12** (71 mg, 12% from crude **45**). ^{1}H NMR (400 MHz, DMSO-d_6) δ 7.98 (m, 1H), 7.70 (m, 1H), 7.28 (m, 2H), 5.60 (m, 1H), 5.40 (d, J = 6.35, 1H), 4.24 (s, br, 4H), 4.05 (s, 1H), 3.81 (s, 3H), 3.78 (m, 4H), 3.73 (s, 2H), 2.90 (d, J = 10.9, 2H), 1.99 (t, J = 10.7, 2H), 1.66 (d, J = 10.4, 2H), 1.61 (d, J = 6.49, 3H), 1.21 (m, 3H), 1.02 (s, 6H). MS (ESI): m/z (M + H)$^+$ 535. Analytical LC-MS on an Agilent 1200 using a 2.1 mm × 30 mm SD-C18 analytical column and H_2O/MeCN modified with 0.05% trifluoroacetic acid, running a linear gradient from 3% MeCN to 95% MeCN, monitoring by a UV wavelength of 254 nm and ESI+ TIC MS, showed 100% purity.

Preparation of 2-(1-((2-(2-Isopropyl-1*H*-benzo[*d*]imidazol-1-yl)-9-methyl-6-morpholino-9*H*-purin-8-yl)methyl)piperidin-4-yl)propan-2-ol (13). Compound **13** was prepared from **36** according to a coupling procedure similar to that described for compound **11**, using 2-isopropyl-1*H*-benzo[*d*]imidazole. Yield = 26%. ^{1}H NMR (400 MHz, DMSO-d_6) δ 7.89 (m, 1H), 7.64 (m, 1H), 7.23 (m, 2H), 4.26 (s, br, 4H), 4.00 (s, 1H), 3.92 (m, 1H), 3.81 (s, 3H), 3.77 (m, 4H), 3.73 (s, 2H), 2.91 (d, J = 11.0, 2H), 2.00 (t, J = 11.3, 2H), 1.66 (d, J = 12.1, 2H), 1.35 (d, J = 6.8, 6H), 1.21 (m, 3H), 1.02 (s, 6H). MS (ESI): m/z (M + H)$^+$ 533. Analytical LC-MS on an Agilent 1200 using a 2.1 mm × 30 mm SD-C18 analytical column and H_2O/MeCN modified with 0.05% trifluoroacetic acid, running a linear gradient from 3% MeCN to 95% MeCN, monitoring by a UV wavelength of 254 nm and ESI+ TIC MS, showed 100% purity.

Preparation of 2-(1-((2-(2-(Dimethylamino)-1*H*-benzo[*d*]-imidazol-1-yl)-9-methyl-6-morpholino-9*H*-purin-8-yl)methyl)-piperidin-4-yl)propan-2-ol (14). Compound **14** was prepared from **36** according to a coupling procedure similar to that described for compound **9**, using *N*,*N*-dimethyl-1*H*-benzo[*d*]imidazol-2-amine. Yield = 38.1%. ^{1}H NMR (400 MHz, DMSO-d_6) δ 7.53 (d, J = 7.76, 1H), 7.30 (d, J = 7.74, 1H), 7.07 (t, J = 7.62, 1H), 6.94 (t, J = 7.62, 1H), 4.21 (s, br, 4H), 4.00 (s, 1H), 3.80 (s, 3H), 3.75 (m, 4H), 3.72 (s, 2H), 2.90 (s, 6H), 1.99 (t, J = 11.2, 2H), 1.66 (d, J = 11.8, 2H), 1.21 (m, 3H), 1.02 (s, 6H). MS (ESI): m/z (M + H)$^+$ 534. Analytical LC-MS on an Agilent 1200 using a 2.1 mm × 30 mm SD-C18 analytical column and H_2O/MeCN modified with 0.05% trifluoroacetic acid, running a linear gradient from 3% MeCN to 95% MeCN, monitoring by a UV wavelength of 254 nm and ESI+ TIC MS, showed 100% purity.

Preparation of 2-(1-((9-Methyl-6-morpholino-2-(2-morpholino-1*H*-benzo[*d*]imidazol-1-yl)-9*H*-purin-8-yl)methyl)-piperidin-4-yl)propan-2-ol (15). Compound **15** was prepared from **36** according to a coupling procedure similar to that described for compound **9**, using 4-(1*H*-benzo[*d*]imidazol-2-yl)morpholine. Yield = 60%. ^{1}H NMR (400 MHz, DMSO-d_6) δ 7.66 (d, J = 7.6, 1H), 7.39 (d, J = 7.6, 1H,), 7.12 (dd, J = 11.4, J = 3.77, 1H), 7.03 (m, 1H), 4.27 (s, br, 4H), 4.02 (s, 1H), 3.82 (s, 3H), 3.76 (m, 4H), 3.72 (s, 2H), 3.64 (m, 4H), 3.23 (m, 4H), 2.90 (d, J = 11.1, 2H), 1.99 (t, J = 10.9, 2H,), 1.66 (d, J = 10.8, 2H), 1.23 (m, 3H), 1.02 (s, 6H). MS (ESI): m/z (M + H)$^+$ 576. Analytical LC-MS on an Agilent 1200 using a 2.1 mm × 30 mm SD-C18 analytical column and H_2O/MeCN modified with 0.05% trifluoroacetic acid, running a linear gradient from 3% MeCN to 95% MeCN, monitoring by a UV wavelength of 254 nm and ESI+ TIC MS, showed 100% purity.

Preparation of 4-(2-(2-Ethyl-1*H*-benzo[*d*]imidazol-1-yl)-9-methyl-8-((4-(methylsulfonyl)piperazin-1-yl)methyl)-9*H*-purin-6-yl)morpholine (16). Compound **16** was prepared according to a procedure similar to that described for compound **3**, using 1-(methylsulfonyl)piperazine. Yield = 77%. ^{1}H NMR (400 MHz, DMSO-d_6) δ 8.01 (m, 1H), 7.63 (m, 1H), 7.24 (m, 2H), 4.26 (s, br, 4H), 3.86 (m, 7H), 3.77 (s, 2H), 3.26 (m, 2H), 3.25 (br, s, 4H), 2.76 (s, 3H), 2.60 (m, 4H), 1.45 (m, 3H). MS (ESI): m/z (M + H)$^+$ 540. Analytical LC-MS on an Agilent 1200 using a 2.1 mm × 30 mm SD-C18 analytical column and H_2O/MeCN modified with 0.05% trifluoroacetic acid, running a linear gradient from 3% MeCN to 95% MeCN, monitoring by a UV wavelength of 254 nm and ESI+ TIC MS, showed 100% purity.

Preparation of 2-(4-((2-(2-Ethyl-1*H*-benzo[*d*]imidazol-1-yl)-9-methyl-6-morpholino-9*H*-purin-8-yl)methyl)piperazin-1-yl)-2-methylpropanamide (17). Compound **17** was prepared according to a procedure similar to that described for compound **3**, using 2-methyl-2-(piperazin-1-yl)propanamide. Yield = 42%. ^{1}H NMR (400 MHz, DMSO-d_6) δ 8.03 (m, 1H), 7.63 (m, 1H), 7.26 (m, 2H), 7.07 (s, 1H), 6.98 (s, 1H), 4.26 (s, 4H), 3.82 (s, 3H), 3.78 (m, 6H), 3.27 (m, 2H), 2.43 (s, br, 4H), 1.34 (t, J = 7.44, 3H), 1.06 (s, 6H). MS (ESI): m/z (M + H)$^+$ 547. Analytical LC-MS on an Agilent 1200 using a 2.1 mm × 30 mm SD-C18 analytical column and H_2O/MeCN modified with 0.05% trifluoroacetic acid, running a linear gradient from 3% MeCN to 95% MeCN, monitoring by a UV wavelength of 254 nm and ESI+ TIC MS, showed 100% purity.

Preparation of 4-(2-(2-Ethyl-1*H*-benzo[*d*]imidazol-1-yl)-9-methyl-8-((4-(methylsulfonyl)piperazin-1-yl)methyl)-9*H*-purin-6-yl)morpholine (18). Compound **18** was prepared according to a procedure similar to that described for compound **3**, using 1-*tert*-butylpiperazine. Yield = 64%. ^{1}H NMR (400 MHz, $CDCl_3$) δ 8.01 (m, 1H), 7.75 (m, 1H), 7.25 (m, 2H), 4.40 (s, br, 4H), 3.85 (m, 7H), 3.77 (s, 2H), 3.40 (m, 2H), 2.60 (s, 8H), 1.40 (m, 3H), 1.02 (s, 9H). MS (ESI): m/z (M + H)$^+$ 518. Analytical LC-MS on an Agilent 1200 using a 2.1 mm × 30 mm SD-C18 analytical column and H_2O/MeCN modified with 0.05% trifluoroacetic acid, running a linear gradient from 3% MeCN to 95% MeCN, monitoring by a UV wavelength of 254 nm and ESI+ TIC MS, showed 100% purity.

Preparation of 2-(2-Ethyl-benzoimidazol-1-yl)-9-methyl-6-morpholin-4-yl-8-((1*S*,4*S*)-5-oxetan-3-yl-2,5-diazabicyclo-[2.2.1]hept-2-ylmethyl)-9*H*-purine (19). To a pressure tube was charged **31** (5.64 g, 20.0 mmol), 2-ethyl-1*H*-benzimdazole (3.21 g, 22.0 mmol), tris(dibenzylideneacetone)dipalladium(0) (0.458 g, 0.5 mmol), XPhos (0.954 g, 2.0 mmol), cesium carbonate (9.78 g, 30.0 mmol), and dioxane (80. mL). The reaction was degassed for 5 min, sealed, and heated at reflux for 18 h. The reaction mixture was then filtered through a pad of Celite while hot, and the pad was washed with hot dioxane. The combined filtrate was concentrated to give a residue which was triturated with Et_2O (100 mL), filtered, and dried under vacuum to give **42** (4.5 g, 58%)

A mixture of **42** (200 mg, 0.51 mmol), **44** (122 mg, 0.62 mmol), and molecular sieves (4 Å, powdered, 520 mg) in DCE (10 mL) was stirred at ambient temperature for 3 h. Sodium triacetoxyborohydride (162 mg, 0.76 mmol) was added and the mixture stirred for 17 h, then loaded onto an Isolute SCX-2 cartridge (25 g). The cartridge was then washed with methanol, and the desired product was subsequently eluted using 2 M NH_3 in MeOH. The eluant was collected and concentrated in vacuo. The resultant residue was purified by flash chromatography (0−15% MeOH in EtOAc) to give **43** as a white solid (294 mg, quant.).

TFA (3 mL) was added to a solution of **43** (294 mg, 0.51 mmol) in DCM (10 mL) and the mixture stirred at ambient temperature for 30 min, then loaded onto an Isolute SCX-2 cartridge (25 g). The cartridge was then washed with methanol, and the desired product was subsequently eluted using 2 M NH_3 in MeOH. The eluant was collected and concentrated in vacuo. The resultant residue was purified by flash chromatography (0−15% MeOH in DCM) to afford 8-[(1*S*,4*S*)-1-(2,5-diazabicyclo[2.2.1]hept-2-yl)methyl]-2-(2-ethylbenzoimidazol-1-yl)-9-methyl-6-morpholin-4-yl-9*H*-purine as a white solid (153 mg, 63%).

A solution of of 8-[(1*S*,4*S*)-1-(2,5-diazabicyclo[2.2.1]hept-2-yl)-methyl]-2-(2-ethyl-benzoimidazol-1-yl)-9-methyl-6-morpholin-4-yl-9*H*-purine (250 mg, 0.53 mmol), oxetan-3-one (40 mg, 0.31 mmol), and molecular sieves (4 Å, powdered, 200 mg) in DCE (7 mL) was stirred at ambient temperature for 4 h. Sodium triacetoxyborohydride

(148 mg, 0.70 mmol) was added and the mixture stirred for 16 h, then loaded onto an Isolute SCX-2 cartridge (10 g). The cartridge was then washed with methanol, and the desired product was subsequently eluted using 2 M NH_3 in MeOH. The eluant was collected and concentrated in vacuo. The resultant residue was purified by flash chromatography (0−10% MeOH in DCM) to afford **19** as a white solid (125 mg, 45%). ^{1}H NMR (400 MHz, $CDCl_3$,) δ 8.02 (m, 1H); 7.76 (m, 1H); 7.26 (m, 2H); 4.72−4.65 (m, 4H); 4.31 (m, 4H); 4.01−3.86 (m, 10H); 3.35 (m, 4H); 2.99 (m, 1H); 2.82 (m, 1H); 2.76 (m, 2H); 1.79 (m, 2H), 1.45 (t, J = 7.5, 3H). MS (ESI): m/z $(M + H)^+$ 530. Analytical LC-MS on an Agilent 1200 using a 2.1 mm × 30 mm SD-C18 analytical column and H_2O/MeCN modified with 0.05% trifluoroacetic acid, running a linear gradient from 3% MeCN to 95% MeCN, monitoring by a UV wavelength of 254 nm and ESI+ TIC MS, showed 100% purity.

Preparation of 4-(1-((2-(2-ethyl-1*H*-benzo[*d*]imidazol-1-yl)-9-methyl-6-morpholino-9*H*-purin-8-yl)methyl)azetidin-3-yl)-morpholine (20). Compound **20** was prepared according to a procedure similar to that described for compound **3**, using 4-azetidin-3-ylmorpholine. Yield = 11%. ^{1}H NMR (400 MHz, $CDCl_3$): δ 8.02−7.98 (m, 1H); 7.77−7.73 (m, 1H); 7.27−7.23 (m, 2H); 4.35 (m, 4H); 3.89−3.82 (m, 6H); 3.83 (s, 3H); 3.72 (m, 4H); 3.56 (m, 2H); 3.34 (q, J = 7.5, 2H); 3.15−3.03 (m, 3H); 2.34 (m, 4H) and 1.44 (t, J = 7.5, 3H). MS (ESI): m/z $(M + H)^+$ 518. Analytical LC-MS on an Agilent 1200 using a 2.1 mm × 30 mm SD-C18 analytical column and H_2O/MeCN modified with 0.05% trifluoroacetic acid, running a linear gradient from 3% MeCN to 95% MeCN, monitoring by a UV wavelength of 254 nm and ESI+ TIC MS, showed 100% purity.

Characterization of Biochemical and Cellular Activity in Vitro. Assays were performed as described previously.[17] Briefly, the enzymatic activity of the Class I PI3K isoforms was measured using a fluorescence polarization assay that monitors formation of the product 3,4,5-inositoltriphosphate molecule as it competes with fluorescently labeled PIP3 for binding to the GRP-1 pleckstrin homology domain protein. An increase in phosphatidyl inositide-3-phosphate product results in a decrease in fluorescence polarization signal as the labeled fluorophore is displaced from the GRP-1 protein binding site. Class I PI3K isoforms were purchased from Millipore or were expressed and purified as heterodimeric recombinant proteins. Tetramethylrhodamine-labeled PIP3 (TAMRA-PIP3), di-C8-PIP2, and PIP3 detection reagents were purchased from Echelon Biosciences. PI3K isoforms were assayed under initial rate conditions in the presence of 10 mM Tris (pH 7.5), 25 μMATP, 9.75 μMPIP, 2,5%glycerol, 4 mMMgCl_2, 50 mMNaCl, 0.05% (v/v) Chaps, 1 mM dithiothreitol, and 2% (v/v) DMSO at the following concentrations for each isoform: PI3Kα,β at 60 ng/mL; PI3Kγ at 8 ng/mL; and PI3Kδ at 45 ng/mL. After assaying for 30 min at 25 °C, reactions were terminated with a final concentration of 9 mM EDTA, 4.5 nM TAMRAPIP3, and 4.2 μg/mL GRP-1 detector protein before reading fluorescence polarization on an Envision plate reader. IC_{50} values were calculated from the fit of the dose−response curves to a 4-parameter equation.

Cellular Assays.[18] Akt (Ser 473) phosphorylation cellular assays were conducted using human B cell lymphoma Ri-1 cells provided by the German Collection of Microorganisms and Cell Cultures (Braunschweig Germany). Cells were cultured in RPMI supplemented with 10% fetal bovine serum, 100 units/mL penicillin, 100 μg/mL streptomycin, 10 mM HEPES, and 2 mM glutamine at 37 °C under 5% CO_2. Cells were seeded in 384-well plates in RPMI media containing 5% human serum albumin and 1 mg/mL α1-acid glycoprotein at 200,000 cells/well prior to the addition of compounds. Test compound or DMSO vehicle of 0.5% v/v was added to the cell mixture and allowed to preincubate for 30 min at 37 °C and 5% CO_2, prior to stimulation with F(ab′)2 Frag Goat antihuman IgM Fc5u (Jackson 109-006-129, 25ug/mL final). Anti-IgM stimulation was allowed to proceed for 1 h at 37 °C and 5% CO_2 then lysed with MSD complete lysis buffer. AKT(Ser473) phosphorylation accumulation from cell lysates was determined by a commercially available sandwich immunoassay developed by MesoScale Discovery (MesoScale #K151CAD, Gaithersburg, MD). IC_{50} values were calculated from the fit of the dose−response curves to a 4-parameter equation.

Inhibition of CD86 Production in Mice Following Anti-IgD Injection with Compound 5. BALB/c mice (4/group) were separated into eight groups. Control groups were treated with saline (po), vehicle (po), and 150 μg/mouse anti-IgD IV + saline (po), or 150 μg/mouse anti-IgD IV + MCT. Compound treated animals were first treated with compound (oral gavage) and, after 0.5 h, injected with 150 μg anti-IgD. Mice were euthanized 6 h after treatment with anti-IgD. Blood was analyzed for B cell numbers and expression of CD86 by FACS.

■ ASSOCIATED CONTENT

Supporting Information

Details of the cocrystal structure of compound **14** with PI3Kγ. This material is available free of charge via the Internet at http://pubs.acs.org.

■ AUTHOR INFORMATION

Corresponding Author

*E-mail: murray.jeremy@gene.com (J.M.M.); zachary.sweeney@novartis.com (Z.K.S.).

Notes

The authors declare no competing financial interest.

■ REFERENCES

(1) Okkenhaug, K.; Vanhaesebroeck, B. PI3K-signalling in B- and T-cells: insights from gene-targeted mice. *Biochem. Soc. Trans.* **2003**, *31*, 270−274.

(2) Okkenhaug, K.; Vanhaesebroeck, B. PI3K in lymphocyte development, differentiation and activation. *Nat. Rev. Immunol.* **2003**, *3*, 317−330.

(3) Rommel, C.; Camps, M.; Ji, H. PI3K delta and PI3K gamma: partners in crime in inflammation in rheumatoid arthritis and beyond? *Nat. Rev. Immunol.* **2007**, *7*, 191−201.

(4) Thomas, M.; Owen, C. Inhibition of PI-3 kinase for treating respiratory disease: good idea or bad idea? *Curr. Opin. Pharmacol.* **2008**, *8*, 267−274.

(5) Williams, O.; Hoouseman, B. T.; Kunkel, E. J.; Aizenstein, B.; Hoffman, R.; Knight, Z. A.; Shokat, K. M. Discovery of dual inhibitors of the immune cell PI3Ks p110delta and p110gamma: a prototype for new anti-inflammatory drugs. *Chem. Biol.* **2010**, *17*, 123−34.

(6) Ihle, N. T.; Powis, G. The biological effects of isoform-specific PI3-kinase inhibition. *Curr. Opin. Drug Discovery Dev.* **2010**, *13*, 41−49.

(7) Folkes, A. J.; Ahmadi, K.; Alderton, W. K.; Alix, S.; Baker, S. J.; Box, G.; Chuckowree, I. S.; Clarke, P. A.; Depledge, P.; Eccles, S. A.; Friedman, L. S.; Hayes, A.; Hancox, T. C.; Kugendradas, A.; Lensun, L.; Moore, P.; Olivero, A. G.; Pang, J.; Patel, S.; Pergl-Wilson, G. H.; Raynaud, F. I.; Robson, A.; Saghir, N.; Salphati, L.; Sohal, S.; Ultsch, M. H.; Valenti, M.; Wallweber, H. J.; Wan, N. C.; Wiesmann, C.; Workman, P.; Zhyvoloup, A.; Zvelebil, M. J.; Shuttleworth, S. J. The identification of 2-(1H-indazol-4-yl)-6-(4-methanesulfonyl-piperazin-1-ylmethyl)-4-morpholin −4-yl-thieno[3,2-d]pyrimidine (GDC-0941) as a potent, selective, orally bioavailable inhibitor of class I PI3 kinase for the treatment of cancer. *J. Med. Chem.* **2008**, *51*, 5522−5532.

(8) Marone, R.; Cmiljanovic, V.; Giese, B.; Wymann, M. P. Targeting phosphoinositide 3-kinase: moving towards therapy. *Biochim. Biophys. Acta* **2008**, *1784*, 159.

(9) Ihle, N. T.; Powis, G. Take your PIK: phosphatidylinositol 3-kinase inhibitors race through the clinic and toward cancer therapy. *Mol. Cancer Ther.* **2009**, *8*, 1−9.

(10) Raynaud, F. I.; Eccles, S. A.; Patel, S.; Alix, S.; Box, G.; Chuckowree, I.; Folkes, A.; Gowan, S.; De Haven Brandon, A.; Di Stefano, F.; Hayes, A.; Henley, A. T.; Lensun, L.; Pergl-Wilson, G.; Robson, A.; Saghir, N.; Zhyvoloup, A.; McDonald, E.; Sheldrake, P.; Shuttleworth, S.; Valenti, M.; Wan, N. C.; Clarke, P. A.; Workman, P. Biological properties of potent inhibitors of class I phosphatidylinosi-

tide 3-kinases: from PI-103 through PI-540, PI-620 to the oral agent GDC-0941. *Mol. Cancer Ther.* **2009**, *8*, 1725−1728.
(11) Sadhu, C.; Masinovsky, B.; Dick, K.; Sowell, C. G.; Staunton, D. E. Essential role of phosphoinositide 3-kinase delta in neutrophil directional movement. *J. Immunol.* **2003**, *170*, 2647−2654.
(12) Williams, R.; Berndt, A.; Miller, S.; Hon, W. C.; Zhang, X. Form and flexibility in phosphoinositide 3-kinases. *Biochem. Soc. Trans.* **2009**, *27*, 615−626.
(13) Berndt, A.; Miller, S.; Williams, O.; Le, D. D.; Houseman, B. T.; Pacold, J. I.; Gorrec, F.; Hon, W. C.; Liu, Y.; Rommel, C.; Gaillard, P.; Ruckle, T.; Schwarz, M. K.; Shokat, K. M.; Shaw, J. P.; Williams, R. L. The p110delta structure: mechanisms for selectivity and potency of new PI3K inhibitors. *Nat. Chem. Biol.* **2010**, *6*, 244.
(14) Zvelebil, M. J.; Waterfield, M. D.; Shuttleworth, S. J. Structural analysis of PI3-kinase isoforms: Identification of residues enabling selective inhibition by small molecule ATP-competitive inhibitors. Arch. *Biochem. Biophys.* **2008**, *477*, 404−410.
(15) Knight, Z. A.; Gonzalez, B; Feldman, M. E.; Zunder, E. R.; Goldenberg, D. D.; Williams, O.; Loewith, R.; Stokoe, D.; Balla, A.; Toth, B.; Balla, T.; Weiss, W. A.; Williams, R. L.; Shokat, K. M. A pharmacological map of the PI3-K family defines a role for p110alpha in insulin signaling. *Cell* **2006**, *125*, 733−47.
(16) Safina, B. S.; Baker, S.; Baumgardner, M.; Blaney, P. M.; Chan, B. K.; Chen, Y.-H.; Cartwright, M. W.; Castanedo, G.; Chabot, C.; Cheguillaume, A. J.; Goldsmith, P.; Goldstein, D. M.; Goyal, B.; Hancox, T.; Handa, R. K.; Iyer, P. S.; Kaur, J.; Kondru, R.; Kenny, J. R.; Krintel, S. L.; Li, J.; Lesnick, J.; Lucas, M. C.; Lewis, C.; Mukadam, S.; Murray, J.; Nadin, A. J.; Nonomiya, J.; Padilla, F.; Palmer, W. S.; Pang, J.; Pegg, N.; Price, S.; Reif, K.; Salphati, L.; Savy, P. A.; Seward, E. M.; Shuttleworth, S.; Sohal, S.; Sweeney, Z. K.; Tay, S.; Tivitmahaisoon, P.; Waszkowycz, B.; Wei, B.; Yue, Q.; Zhang, C.; Sutherlin, D. P. Discovery of novel PI3-kinase δ specific inhibitors for the treatment of rheumatoid arthritis: taming CYP3A4 time-dependent inhibition. *J. Med. Chem.* **2012**, *55*, 5887−5900.
(17) Sutherlin, D. P.; Sampath, D.; Berry, M.; Castanedo, G.; Chang, Z.; Chuckowree, I.; Dotson, J.; Folkes, A.; Friedman, L.; Goldsmith, R.; Heffron, T.; Lee, L.; Lesnick, J.; Lewis, C.; Mathieu, S.; Nonomiya, J.; Olivero, A.; Pang, J.; Prior, W. W.; Salphati, L.; Sideris, S.; Tian, Q.; Tsui, V.; Wan, N. C.; Wang, S.; Wiesmann, C.; Wong, S.; Zhu, B. Y. Discovery of (thienopyrimidin-2-yl)aminopyrimidines as potent, selective, and orally available pan-PI3-kinase and dual pan-PI3-kinase/mTOR inhibitors for the treatment of cancer. *J. Med. Chem.* **2010**, *53*, 1086−1097.
(18) Lesnick, J. et al., manuscript in preparation.
(19) (a) Peters, J.-U.; Schnider, P.; Mattei, P.; Kansy, M. Pharmacological promiscuity: dependence on compound properties and target specificity in a set of recent Roche compounds. *ChemMedChem* **2009**, *4*, 680−686. (b) Avdeef, A; Artursson, P.; Neuhoff, S.; Lazorova, L.; Grasjo, J.; Tavelin, S. Caco-2 permeability of weakly basic drugs predicted with the double-sink PAMPA pKa(flux) method. *Eur. J. Pharm. Sci.* **2005**, *4*, 333−349.
(20) Calculations were performed using Schrodinger/Jaguar software. Using default parameters, relaxed coordinate scans were made using DFT:B3LYP/6-31G** with default parameters.
(21) See the Supporting Information for structural details.
(22) The model was generated by docking 19 into the crystal structure of p110d in complex with GDC-0941 (PDB ID 2WXP).
(23) Compounds were tested for inhibition of CYP1A2, CYP3A4, CYP2C9, CYP2C19, and CYP2D6.
(24) Testing performed using Invitrogen SelectScreen Kinase Profiling Service.
(25) Kasprowicz, D. J.; Kohm, A. P.; Berton, M. T.; Chruscinski, A. J.; Sharpe, A.; Sanders, V. M. Stimulation of the B cell receptor, CD86 (B7−2), and the b_2-adrenergic receptor intrinsically modulates the level of IgG1 and IgE produced per B cell. *J. Immunol.* **2000**, *165*, 680−690.